Received 31 October 2022; revised 2 December 2022; accepted 25 December 2022. Date of publication 3 February 2023; date of current version 14 April 2023.

Digital Object Identifier 10.1109/OJCOMS.2023.3240116

Performance Analysis of Spectrum Sharing Radar in Multipath Environment

GUNNERY SRINATH [1] (Graduate Student Member, IEEE), BETHI PARDHASARADHI [1] (Member, IEEE), ASHOKA CHAKRAVARTHI MAHIPATHI [2] (Graduate Student Member, IEEE), PRASHANTHA KUMAR H [2], PATHIPATI SRIHARI [2] (Senior Member, IEEE), AND LINGA REDDY CENKERAMADDI [3] (Senior Member, IEEE)

[1]Department of Advanced Driver Assistant Systems, Continental Automotive Components (India) Pvt., Ltd., Bengaluru 560100, India

[2]Department of Electronics and Communication Engineering, National Institute of Technology Karnataka, Surathkal 575025, India

[3]Department of Information and Communication Technology, University of Agder, 4879 Grimstad, Norway

CORRESPONDING AUTHOR: P. SRIHARI (e-mail: srihari.js@gmail.com)

This work was supported by the National Institute of Technology Karnataka, University Grants Commission of India.

ABSTRACT Radar based sensing and communication systems sharing a common spectrum have become a potential research problem in recent years due to spectrum scarcity. The spectrum sharing radar (SSR) is a new technology that uses the total available bandwidth (BW) for both radar based sensing and communication. Unlike traditional radar, the SSR divides the total available BW into radar-only and mixed-use bands. In a radar-only band, only radar sensor signals can be transmitted and received. In contrast, radar and communication signals can both be transmitted and received in the mixed-use band. Taking such BW sharing into account, this paper investigates the performance of SSR in an information-theoretic sense. To evaluate performance, mutual information (MI), spectral efficiency (SE) and capacity (C) metrics are used. Initially, this paper considered a clean environment (no multipath) in order to evaluate performance metrics in the mixed-use band with and without successive interference cancellation. Following that, this paper addresses the performance of BW allocation by allocating low to high BW in mixed-band. Furthermore, the performance metrics are extended to account for the multipath environment, and the same analogy as in a clean environment is used. In addition, the MI and SE of traditional radar system is taken into account when comparing the performance of SSR with and without the use of the SIC. Finally, MI and capacity results show that using the SIC scheme in a mixed-use band yields performance comparable to traditional radar and communication system. In terms of SE, the SSR with SIC scheme outperforms traditional radar and communication system.

INDEX TERMS Communication system, interference, mutual information, performance analysis, radar sensor, spectral efficiency, spectrum sharing.

I. INTRODUCTION

THE USAGE of wireless devices and services is increasing at an exponential rate across the world, which results in the shortage of allotted spectrum for wireless applications [1]. On the other hand, the allocated frequency spectrum of traditional radar varies from lower to higher frequency ranges and is underutilized. Sharing the spectrum between the radar and communication systems leads to effective spectrum utilization for various wireless applications [2], [3], [4], [5].

Many research contributions have been carried out towards radar and communication spectrum sharing. The fundamental concepts of radar and communication system spectrum sharing in [5], [6]. The statistical model for in-band wireless communication interference is developed, and its effect on the radar sensor constant false alarm rate (CFAR) detector is shown [7]. Further, considering the radar and communication system spectrum sharing scenario, examined the effect of radar sensor interference on the communication system and the effect of communication interference on radar system

in terms of standard bounds [8]. The bounds include bit error rate (BER), constellation diagrams, Shannon capacity for the communication system, and receiver operating characteristic curves (ROC) for radar systems. A survey on signal processing strategies for convergence of RF communication and sensing is given in [9]. Further, various optimal waveform design approaches for joint communication and radar system are presented in [4], [10], [11], [12], [13]. Considering the multi-antenna rate splitting mechanism at the transmitter end and successive interference cancellation (SIC) at the receiver section, in [14] the interference management strategies for joint communication and radar system to improve the performance of both the systems simultaneously is presented. Besides, a temporal signal processing algorithm for the detection of radar targets in the presence of in-band communication interference is given in [15]. The algorithm includes the novel frequency shift filter-based whitening filter followed by a matched filter. In [16], a null-space projection based waveform design is considered for radar and communication system spectrum sharing and derived the generalized likelihood ratio test for target detection. A novel frequency-shared weather radar networked system (WRNS) is proposed in [17] to improve the efficiency in frequency/ spectral usage. To improve the capacity of unmanned aerial vehicle (UAV) networks, the spectrum sharing between wireless unmanned aerial vehicle (UAV) mesh networks and ground networks is studied in [18]. To increase the capacity of a code division multiple access (CDMA) system and to reduce the near/far effect, a simple SIC is introduced in [19]. Further, the work in [19] is extended for multiuser detection by considering the multipath fading into account. In [20], the investigation of the SIC method for non-orthogonal multiple access (NOMA) systems is presented. Radar sensor waveform design to maximize the mutual information (MI) with a constraint on both transmit power allocation and maximum target scattering response is illustrated in [21]. In addition to the above contributions, the RadCom also experienced the areas like detection and multi-target tracking in the presence of in-Band wireless interference [22], [23].

In another contribution, the optimal waveform design for multi-input multi-output (MIMO) based joint radar and communication system framework with the constraint on MI maximization is presented [24]. The radar and communication spectrum sharing is also addressed from an automotive application perspective [25], [26], [27]. In addition, by considering constraints as a spectral shape, autocorrelation, peak side-lobe-to-main-lobe ratio, radar sensor waveform spectral leakage, and minimum estimation error variance, [28] presents the radar waveform design for joint/ cooperative radar and communication system. The dual-function radar communication (DFRC) systems use the same hardware and resources for both communication, and radar-like functionality are presented in [29], [30], [31], [32]. In [2] and [33], a thorough literature survey related to radar and communication system spectrum sharing is presented. In the form of communication information rate and the novel radar estimation rate, the authors in [34] have formulated the inner bounds on the performance of radar and communication system spectrum sharing. The target estimation performance improvement in cooperative radar and communication system spectrum sharing presented in [35]. Furthermore, in [36], the performance is evaluated in the form of a localization estimation rate and communication data rate by considering the three different cases (isolated sub-band (ISB), communication isolated sub-band (CIB), and radar isolated sub-band (RIB) situation). Considering the joint radar and communication system (JRCS), the performance is analyzed in the form of Mutual Information (MI) between the radar sensor and the target and the communication data rate [37]. The radar and communication system spectrum sharing research falls in line with the coexistence problem in traditional cellular networks such as cognitive radio [38]. However, the key difference lies in the simultaneous operation of both sensing and communication system functionalities in the same band. Further, it is also capable of bringing the single hardware for possessing both the functionalities. The current research trends in radar and communication system spectrum sharing aimed at making the dual-function radar-communication (DFRC) system a reality [2], [5], [29].

The spectrum sharing radar (SSR) is an dual-function radar-communication (DFRC) system, capable of utilizing the same BW for both radar and communication purposes. Since, the DFRC systems are becoming popular [29], [31], [39], [40], there is a need to analyse the performance of such systems. Therefore, this paper considers SSR in a clean environment (without multipath), assuming that the total BW is split for radar-only and mixed-use purposes and analyzes its performance in an information theoretic perspective. The SSR performance is analyzed using MI and SE metrics from the radar perspective in an information-theoretic sense and capacity (C) metric is considered from communication perspective. First, the MI of SSR is evaluated for the allocated radar-only BW. In addition, we considered the mixed-band BW along with radar-only BW to obtain the overall MI of the SSR. Hence, the total MI is calculated in two different cases, namely, 1. the radar-only MI and MI with SIC in mixed-use 2. radar-only MI and MI without SIC in mixed-use. In addition to MI, we introduced the SE metric to evaluate the spectral utilization of the SSR. Initially, the SE is evaluated to the radar-only BW. After that, to evaluate overall SE, two different cases are considered, namely 1. the radar-only SE and SE with SIC in mixed-use 2. radar-only SE and SE without SIC in mixed-use. In contrast to MI and SE, the communication C is calculated for the mixed-use band (since it is the only band, which carries communication system information). To comprehensively look into the problem, the multipath environment between the target-to-receiver of SSR is also incorporated and evaluated the SSR performance pertaining to MI, SE, and C. Finally, the performance of the SSR is compared with the traditional radar and communication system.

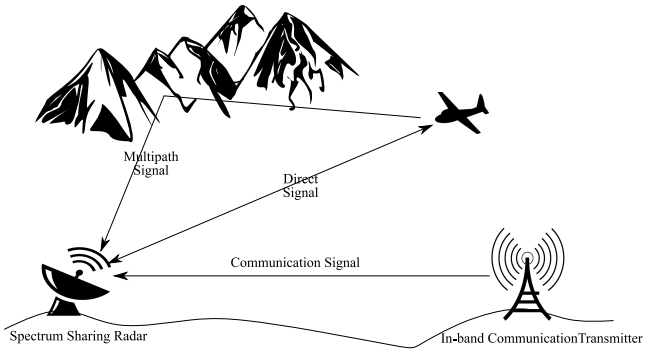

FIGURE 1. System model of a spectrum sharing radar.

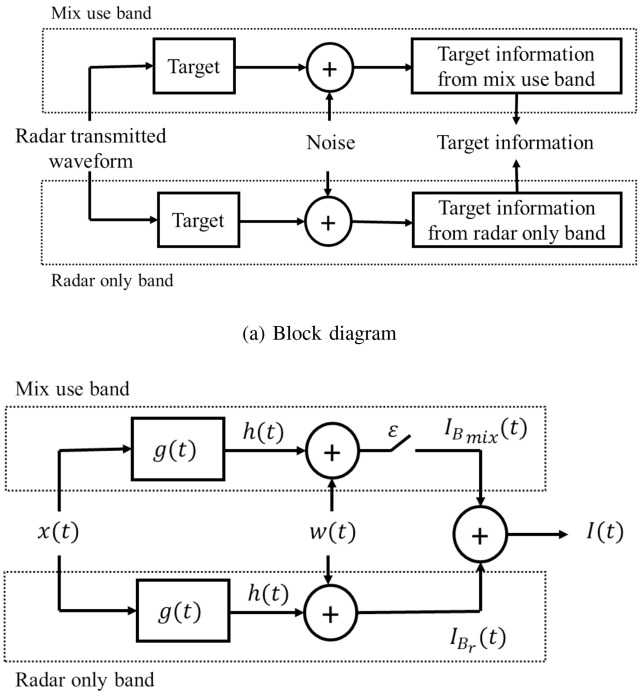

FIGURE 2. Spectrum sharing radar target-to-receiver channel model.

The key contributions of the paper are as follows:

- The SSR performance is analyzed using MI and SE metrics from the radar perspective, considering capacity (C) metric from the communication perspective, assuming that the SSR BW split among the radar-only and mixed-use.
- The overall MI of SSR is calculated as a summation of MI in radar-only band plus MI in mixed usage band. The mixed usage band MI is further evaluated using with/without SIC. The metric is compared against the traditional radar.
- Similar to MI, the overall SE of the SSR is also calculated and compared with traditional radar.
- The capacity metric of SSR is also calculated in mixed-use band and compared with traditional communication system.
- Moreover, the multipath environment between the target-to-receiver channel of SSR is modeled to see the feasibility of the proposed metric in real-time assumptions.

The rest of the paper is organized as follows. Section II presents the Problem formulation to consider MI, SE, and C metrics in SSR. The performance analysis of SSR corresponding to clean environment is presented in Section III. Thereafter, the multipath environment is considered, and performance evaluation is given in Section IV. Finally, the numerical results and conclusions of the work are presented in Sections V and VI respectively.

II. PROBLEM FORMULATION

Let us consider an SSR, where the SSR is detecting the targets and simultaneously acting as a communication receiver as shown in Figure 1. It is assumed that total available bandwidth (B_{SSR}) of the SSR split among radar only sub-band with bandwidth (B_r) and mixed-use bandwidth (B_{mix}). Here, mixed-use refers to both radar and communication purposes. The SSR is capable of extracting the target information from the radar-only sub-band. Meanwhile, the mixed-use band is for both target information and communication data. Since this paper analyses the performance from the radar perspective, Figure 2(a) illustrates the radar target channel model of SSR from the information-theoretic viewpoint. The radar sensor transmitted waveform $x(t)$ impinges on the target and gets scattered by it. The scattered signal with additive noise received at the SSR receiver and further processed to extract the target information from radar-only and mixed-use bands. The target-to-receiver channel equivalent mathematical model is shown in Figure 2(b), where $x(t)$ is the radar sensor transmitted waveform, with duration T having the energy E_x. The $g(t)$ is the target scattering characteristics model/ impulse response; $h(t)$ is the resulting target scattered signal. The $w(t)$ is the zero-mean white Gaussian noise having the power spectral density P_{ww}, which is independent of $x(t)$ and $g(t)$. The $w(t)$ is represented with an intent that the overall SSR system bandwidth ($B_{SSR} = B_r + B_{mix}$) is influenced by the same noise. The ϵ quantifies the loss of target information in the received signal owing to in-band communication interference for the mixed band system operation. The received signal/ measurement model at the radar receiver from the radar only sub-band is given by [41]

$$\begin{aligned} z_r(t; B_r) &= f(h(t), x(t), g(t)) + w(t) \\ &= \sqrt{P_r} s_r(t-\tau) + w(t). \end{aligned} \tag{1}$$

Here, $f(\cdot)$ represents the non-linear function and t represents the time, P_r is radar received power due to target return. Whereas the received signal/ measurement model from the mixed-use sub-band is represented as

$$\begin{aligned} z_r(t; B_{mix}) &= f(h(t), x(t), \epsilon, g(t)) + w(t) \\ &= \sqrt{P_r} s_r(t-\tau) + \sqrt{P_c} s_c(t) + w(t), \end{aligned} \tag{2}$$

where P_c is radar received power owing to in-band communication transmitter, ϵ is a Bernoulli random variable which quantifies the effect of the target information reduction in mixed-use sub-band. The ϵ equal to zero when there is no target information is extracted in mixed-use-band, ϵ takes the value to unity when the target information is extracted.

For the mixed-use sub-band, two cases have been assumed: with SIC and without SIC. It is assumed that, when the SIC method is used, the received signal at the radar receiver will get suppressed with predicted communication symbols. Hence, it cancels the in-band interference effect in mixed-use band [19], [42], [43]. Therefore, the received signal with SIC in mixed band from radar perspective is given by

$$\begin{aligned} z_{r_{SIC}}(t; B_{mix}) &= f(h(t), x(t), \epsilon, g(t)) + w(t) \\ &= \sqrt{P_r} s_r(t-\tau) + \sqrt{P_c}\big(s_c(t) - s_{c_{pre}}(t)\big) + w(t) \\ &= \sqrt{P_r} s_r(t-\tau) + w_{int+n}(t), \end{aligned} \tag{3}$$

where $w_{int+n}(t) = w_{residual}(t) + w(t)$. Here, "*int*" refers to in-band interference, "*n*" refers to noise. Whereas, mixed-use band without SIC will not predict and suppress the in-band communication symbols, results in strong in-band interference effect, which nullifies target information in that particular sub-band. Therefore, the received signal without SIC in mixed band is same as (3) with $w_{int+n}(t) = \sqrt{P_c} s_c(t) + w(t)$. Similar equation holds true from communication perspective in mixed-used band by interchanging the radar and communication signals in (3).

The received signals $z_r(t; B_r), z_r(t; B_{mix})$ given in (1) and (2) are processed to extract the target information. Let $I_{B_r}(t)$ and $I_{B_{mix}}(t)$ be the extracted target information from radar only sub-band and mixed-use sub-band, respectively. So, the overall target information $I_{\text{SSR}}(t)$ from both the sub-bands is the summation of $I_{B_{mix}}(t)$ and $I_{B_r}(t)$. To make the target-to-receiver channel model more realistic, it is also assumed that there exists multipath between the target-to-receiver channel, as shown in Figure 1. The mathematical representation of the multipath model of SSR in radar only band is shown in Figure 3. A similar figure holds true for the mixed-use band, and ϵ exists. N number of paths between the target-to-receiver are depicted in Figure 3. These multipaths are effected by noise $w(t) = f(w_1(t), \ldots, w_n(t))$. Here, $w_1(t), w_2(t), \ldots, w_n(t)$ are the individual path noise components represented for mathematical convenience and are jointly contributing to a single noise component $w(t)$. Further, for simplicity, it is assumed that all the multipaths have a unity channel gain. By imposing subscript i to the (1), (2), results in received signal of i^{th} path. The overall received signal at the radar receiver due to multipath from the radar only and mixed-use sub-band, is given by

$$\begin{aligned} z_r(t; B_r) &= \sum_{i=1}^{N} z_{r_i}(t; B_r), \\ z_r(t; B_{mix}) &= \sum_{i=1}^{N} z_{r_i}(t; B_{mix}). \end{aligned} \tag{4}$$

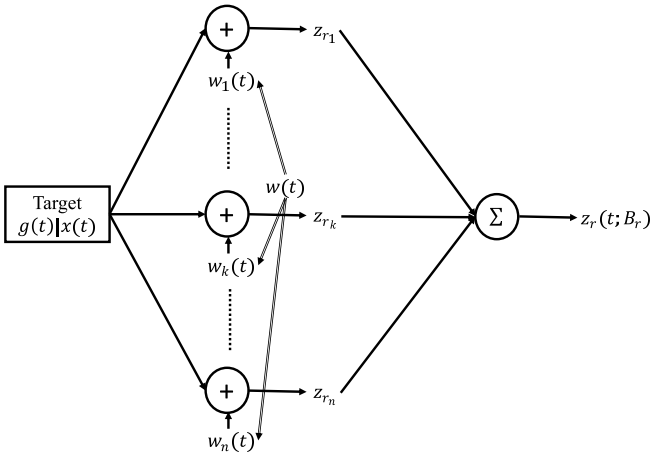

FIGURE 3. Multipath target-to-receiver channel model of spectrum sharing radar in radar only band.

Here, It is worth noting that $z_{r_i}(t; B_r)$, $z_{r_i}(t; B_{mix})$ are equivalent to (1) and (2) for single path.

In the above scenario, there is a strong need to quantify the target information available at the radar for a given transmitted waveform. Besides, SSR is also capable of acting as a communication receiver. Here, there is a strong requirement to estimate the information rate at the SSR. Similarly, it is essential to quantify how efficiently the SSR utilizes the spectrum. Given this, the performance analysis of SSR is carried out using three metrics, namely, mutual information (MI), spectral efficiency (SE), and capacity (C). MI is considered for target-to-receiver channel for a given transmitted waveform to quantify the target information that is available at the radar. Furthermore, as the MI defines the target information available at the receiver, which in turn influence the other performance metric, such as Cramer-Rao Lower Bound (CRLB). Since, the CRLB is inversely proportional to Fisher information [42], [44]. The SE is adopted in this paper to quantify how efficiently the spectrum is being utilized with the spectrum sharing radar. Finally, the capacity (C) metric is introduced to quantify the communication information rate at SSR.

The following, Sections III and IV, presents the performance analysis of the SSR in a clean and multipath environment.

III. PERFORMANCE ANALYSIS IN A CLEAN ENVIRONMENT

In this section, the performance analysis of SSR in a clean environment is presented using MI, SE, and C metrics.

A. MUTUAL INFORMATION (MI)

The total MI between the target characteristics $g(t)$ and the received signal at the radar receiver $z_r(t)$ over a bandwidth B_{SSR} is the summation of the MI in radar only band $I_{B_r}(t)$ and the MI in mixed-use band $I_{B_{mix}}(t)$. Here $B_{SSR} = B_r + B_{mix}$.

1) MI IN RADAR-ONLY BAND

Let $x(t)$ is the radar transmitted waveform with the energy E_x and period T. The MI $(I_{B_r}(z_r(t); g(t) \mid x(t)))$ between the target-to-receiver in the presence of additive Gaussian noise (with $P_{ww}(f)$ as a one sided power spectral density) is maximized by $x(t)$ with magnitude squared spectrum [41]

$$|X(f)|^2 = \max\big[0, A - r(f)\big], \tag{5}$$

where

$$r(f) = \frac{P_{ww}(f)T}{2\sigma_G^2(f)}, \tag{6}$$

$\sigma_G^2(f)$ is spectral variance of $g(t)$, and A is the solution of the equation

$$E_x = \int_{B_r} \max\big[0, A - r(f)\big]\, df, \tag{7}$$

with $r(f)$ defined in (6).

The resulting maximum MI $I_{B_r}^{max}(z_r(t); g(t) \mid x(t))$ over the radar only band interval $B_r = [f_c, f_c + B_r]$ is given by [41], [44], [45]

$$\begin{aligned} I_{B_r}^{max}(z_r(t); g(t)|\, x(t)) &= T\int_{B_r} \ln\left[1 + \frac{2|X(f)|^2\sigma_G^2(f)}{P_{ww}(f)T}\right] df \\ &= T\int_{B_r} \max\big[0, \ln A - \ln r(f)\big]\, df \\ &= TB_r \ln A - T\int_{B_r} \ln r(f)\, df \ \text{(nats)}. \end{aligned} \tag{8}$$

Here, $\frac{2|X(f)|^2\sigma_G^2(f)}{P_{ww}(f)T}$ represents the signal to noise ratio (SNR) in radar only sub-band, represented as

$$\text{SNR}_{B_r} = \frac{|X(f)|^2\sigma_G^2(f)/T}{P_{ww}(f)/2} \tag{9}$$

2) MI IN MIXED-USE BAND

The MI in the mixed-use sub-band follows the similar procedure of radar-only band, except that, one needs to take the expectation over the variable ϵ, which incorporates the effect of in-band communication system interference. Therefore, the MI $I_{B_{mix}}^{max}(z_r(t); g(t) \mid x(t))$ over the mixed-use band interval $B_{mix} = [f_c, f_c + B_{mix}]$ is given by

$$\begin{aligned} I_{B_{mix}}^{max}(z_r(t); g(t)|\, x(t)) &= \mathop{\mathbb{E}}_{\epsilon}\big[I_{B_{mix}}^{max}(z_r(t); g(t) \mid x(t), \epsilon)\big] \\ &= 0 \times p(\epsilon = 0) I_{B_{mix}}^{max}(z_r(t); g(t) \mid x(t), \epsilon = 0) \\ &\quad + 1 \times p(\epsilon = 1) I_{B_r}^{max}(z_r(t); g(t) \mid x(t), \epsilon = 1) \\ &= p(\epsilon = 1) I_{B_r}^{max}(z_r(t); g(t) \mid x(t)). \end{aligned} \tag{10}$$

Here, $p(\epsilon = 1)$ represents the mean value of ϵ, takes the values between zero to one. It can be interpreted as an information reduction factor in the mixed-use band compared to the radar-only sub-band.

Similar to (8), the general MI in mixed-use sub-band is given by

$$I_{B_{mix}}^{max}(z_r(t); g(t) \mid x(t)) \propto \ln\big(1 + \text{SINR}_{B_{mix}}\big) \tag{11}$$

Interpreting (10), (11), utilizing expressions (8) and (9), the mean ϵ can be defined as the ratio of signal to interference plus noise ratio (SINR) in mixed-use sub-band ($\text{SINR}_{B_{mix}}$) to the SNR in radar-only sub-band (SNR_{B_r}). However, in contrast to SNR_{B_r}, the $\text{SINR}_{B_{mix}}$ takes two forms. One without using the SIC scheme and the other is using the SIC scheme in mixed-use band [37]. Similar to (9), the $\text{SINR}_{B_{mix}}$ without using SIC scheme is given by

$$\text{SINR}_{B_{mix}}^{\text{without SIC}} = \frac{|X(f)|^2\sigma_G^2(f)/T}{P_{ww}(f)/2 + |S_c(f)|^2}, \tag{12}$$

where $|S_c(f)|^2$ $(P_c = \int_{B_{mix}} |S_c(f)|^2 df)$ denotes the in-band wireless communication transmitter power component. In contrast to (9), the additional term $|S_c(f)|^2$ in the denominator of (12) denotes the direct interference component.

Using the SIC scheme in mixed-use band subtract the received signal with predicted communication component (as represented in (3)). Hence, the resultant $\text{SINR}_{B_{mix}}$ using SIC scheme in mixed-use band is given by

$$\text{SINR}_{B_{mix}}^{\text{with SIC}} = \frac{|X(f)|^2\sigma_G^2(f)/T}{P_{ww}(f)/2 + |S_c^{res}(f)|^2}, \tag{13}$$

where $|S_c^{res}(f)|^2 = |S_c(f) - S_{c_{pre}}(f)|^2$ represents the residual communication power component.

Using (12) and (9), the ratio of $\text{SINR}_{B_{mix}}^{\text{without SIC}}$ to SNR_{B_r} is assumed as $\bar{\epsilon}_1$, given by

$$\bar{\epsilon}_1 = \frac{P_{ww}(f)}{P_{ww}(f) + 2|S_c(f)|^2}. \tag{14}$$

Here, the denominator of $\bar{\epsilon}_1$ has the direct interference component of high value compared to noise, it is approximately equal to zero. It is in fact true that for a fixed value of noise power P_{ww}, (14) becomes $\bar{\epsilon}_1 = \frac{\text{constant}}{\text{constant+high value}} \approx 0$. Which indicates the minimum information retrieval in mixed-use band when SIC scheme is not adopted. Also, the ratio of $\text{SINR}_{B_{mix}}^{\text{with SIC}}$ to SNR_{B_r} is assumed as $\bar{\epsilon}_2$, given by

$$\bar{\epsilon}_2 = \frac{P_{ww}(f)}{P_{ww}(f) + 2|S_c^{res}(f)|^2}, \tag{15}$$

which is approximately equal to one because the denominator will only have residual interference component of less value compared to noise. Therefore, without loss of generality, using (10), (14), and (15) the MI in the mixed-use band is given by

$$I_{B_{mix}}^{max}(z_r(t); g(t) \mid x(t)) = \begin{cases} \bar{\epsilon}_1 & \left(TB_{mix}\ln A - T\int_{B_{mix}} \ln r(f)\, df\right) \\ & \text{without SIC scheme} \\ \bar{\epsilon}_2 & \left(TB_{mix}\ln A - T\int_{B_{mix}} \ln r(f)\, df\right) \\ & \text{with SIC scheme} \end{cases} \tag{16}$$

Finally, the MI of the SSR is the sum of individual MI's in their respective sub-bands, is given by

$$\begin{aligned} I_{B_{SSR}}^{max}(z_r(t); g(t) \mid x(t)) &= I_{B_r}^{max}(z_r(t); g(t) \mid x(t)) \\ &\quad + I_{B_{mix}}^{max}(z_r(t); g(t) \mid x(t)). \end{aligned} \tag{17}$$

Here $I_{B_r}^{max}$ and $I_{B_{mix}}^{max}$ are defined in (8) and (16), respectively.

To show the comparison of the SSR with the traditional radar, MI of the traditional radar having BW (B_T) [41] is given by

$$I_{B_T}^{max}(z_r(t); g(t) \mid x(t)) = T \int_{B_T} \max\left[0, \ln A - \ln r(f)\right] df(\text{nats}), \quad (18)$$

where $r(f)$ and A have the similar form of (6) and (7) by replacing B_r with B_T.

B. SPECTRAL EFFICIENCY (SE)

In this subsection, the SE performance metric for SSR is presented. The SE is defined as a ratio of maximum MI between target-to-receiver of the SSR over the available bandwidth [46], [47]. Therefore, the SE of the SSR is given by

$$\text{SE}_{SSR} = \frac{I_{B_{\text{SSR}}}^{\max}}{B_{\text{SSR}}}, \quad (19)$$

where $I_{B_{\text{SSR}}}^{\max}$ is given in (17) and B_{SSR} is the bandwidth (BW) used by SSR, defined as $B_{\text{SSR}} = B_r + B_{mix}$.

To show the advantage of SSR over the traditional radar in-terms of SE, the SE of the traditional radar is also defined and is given by

$$\text{SE}_T = \frac{I_{B_T}^{\max}}{B_T + B_{mix}}, \quad (20)$$

where $I_{B_T}^{\max}$ is given in (18). The additional BW B_{mix} to the B_T is considered in the denominator instead of taking the $2B_T$. Because, in traditional radar and communication system operation, where the spectrum sharing (SS) is not considered, a BW of B_r is used for radar purpose alone, and an extra BW of B_c is used for communication operation. Here, in SSR, the B_{mix} is the portion of BW which contains the communication information. Therefore, the net effective BW is $B_T + B_{mix}$ with the condition that $B_r = B_T$, and $B_c = B_{mix}$.

It is to be noted that the (19) shows the SE of SSR from the radar perspective. However, apart from radar target information, the SSR also receives the communication information in mixed-use band. Therefore, the SE of SSR from communication system perspective also needs to be quantified. It is known that the SE of communication system is the ratio of Capacity (C) to the BW used [45], the SSR does not use any additional BW (zero B_c) for communication information retrieval, results into a infinite SE.

C. CAPACITY (C) IN MIXED-USE BAND

In this subsection, the channel capacity calculation for SSR is presented. As, the mixed-use band of SSR consist of communication information apart from radar related information, therefore the capacity metric needs to be evaluated in this band. In general, the bandlimited Gaussian channel capacity with a BW $\mathcal{B}$, noise power spectral density of $P_{ww}/2$ watts/Hz, and power P_c watts is defined as [45]

$$C = \mathcal{B} \ln\left(1 + \frac{P_c}{P_{ww}\mathcal{B}}\right) \quad (21)$$

In SSR, B_{mix} is the amount of BW which carries the communication information. Hence, the capacity of traditional communication system with a BW B_{mix} is taken for comparison purpose, it follows (21) by replacing $\mathcal{B}$ with B_{mix}.

Similar to (16), the capacity of SSR in mixed-use band is given by

$$C_{B_{mix}} = \begin{cases} \bar{\epsilon}_1 \quad B_{mix} \ln\left(1 + \frac{P_c}{P_{ww}B_{mix}}\right) \\ \qquad\qquad \text{without SIC scheme} \\ \bar{\epsilon}_2 \quad B_{mix} \ln\left(1 + \frac{P_c}{P_{ww}B_{mix}}\right) \\ \qquad\qquad \text{with SIC scheme.} \end{cases} \quad (22)$$

Here, $\bar{\epsilon}_1$ and $\bar{\epsilon}_2$ are different from MI calculations of the radar case that are presented in Section III-A.2. As the communication perspective is considered here, the radar component is treated as an interference. Therefore, similar to (14) and (15), the corresponding $\bar{\epsilon}_1$ and $\bar{\epsilon}_2$ is given by

$$\bar{\epsilon}_1 = \frac{P_{ww}}{P_{ww} + 2P_r}, \qquad \bar{\epsilon}_2 = \frac{P_{ww}}{P_{ww} + 2P_r^{res}}. \quad (23)$$

Here, $P_r = |X(f)|^2\sigma_G^2(f)/T$ radar power component, $P_r^{res} = P_r - P_{r_{pre}}$ represents the residual radar power component using SIC scheme in the mixed-use band. In addition, the $\bar{\epsilon}_1$ is approximately equal to zero, as the denominator component has the higher interference (radar power) value compared to the noise power. Which provides reduction in the capacity in mixed-use band, when SIC scheme is not deployed. In contrast, $\bar{\epsilon}_2$ is approximately equal to one, because the denominator component consist of insignificant interference residual component compared to noise power.

IV. PERFORMANCE ANALYSIS IN A MULTIPATH ENVIRONMENT

In this section, the performance analysis of SSR is presented by considering the multipath. For mathematical simplicity, assume only two paths, i.e., $i = 1, 2$. Then the reduced channel model has paths with $w_1(t)$, $w_2(t)$ as noise components. Noise components $w_1(t)$, $w_2(t)$ are jointly Gaussian with zero mean and covariance $K_w = \begin{bmatrix} \sigma_w^2 & \rho\sigma_w^2 \\ \rho\sigma_w^2 & \sigma_w^2 \end{bmatrix}$. Where $\sigma_w^2 = \frac{P_{ww}(f)}{2}$, ρ is the correlation coefficient.

A. MI IN A MULTIPATH ENVIRONMENT

In this subsection, the multipath is considered in the derivation of MI of the SSR.

1) MI IN RADAR-ONLY BAND

For the radar transmitted waveform $x(t)$, the MI between the target that has response characteristics $g(t)$ and the receiver

with the reduced multipath model that has $w_1(t)$, $w_2(t)$ as jointly Gaussian in radar only band is given by [45]

$$I_{B_r}(z_r(t); g(t) \mid x(t)) = \frac{1}{2}\ln\left[1 + \frac{2P}{\sigma_{ww}^2(1+\rho)}\right], \quad (24)$$

where P is the power component which represents the target information, is given by $P = \frac{|X(f)|^2\sigma_G^2(f)}{T}$. After substituting P and σ_{ww}^2 in (24), the resulting MI is given by

$$I_{B_r}(z_r(t); g(t) \mid x(t)) = \frac{1}{2}\ln\left[1 + \frac{4|X(f)|^2\sigma_G^2(f)}{P_{ww}(f)T(1+\rho)}\right]. \quad (25)$$

Using (25), the resulting MI $I_{B_r}(z_r(t); g(t) \mid x(t))$, over the radar only band interval $B_r = [f_c, f_c + B_r]$, with multipath effect, is given by

$$I_{B_r}(z_r(t); g(t) \mid x(t)) = T\int_{B_r} \ln\left[1 + \frac{4|X(f)|^2\sigma_G^2(f)}{P_{ww}(f)T(1+\rho)}\right]df \text{(nats)}. \quad (26)$$

Similar to (8), the maximum MI of $I_{B_r}(z_r(t); g(t) \mid x(t))$ in multipath case, with the constraint on transmitted waveform energy E_x, is given by

$$I_{B_r}^{max}(z_r(t); g(t) \mid x(t)) = TB_r \ln D - T\int_{B_r} \ln\left[r(f)\left(\frac{1+\rho}{2}\right)\right]df \text{ (nats)}. \quad (27)$$

The detailed proof of obtaining the maximum $I_{B_r}(z_r(t); g(t) \mid x(t))$ is provided in the Appendix.

For different values of correlation coefficient $\rho = 0, 1, -1$, the resulting MI is given by

$$I_{B_r}^{max}(z_r(t); g(t) \mid x(t)) = \begin{cases} TB_r \ln D - T\int_{B_r} \ln\left[\frac{r(f)}{2}\right] & \text{for } \rho = 0 \\ TB_r \ln D - T\int_{B_r} \ln r(f) & \text{for } \rho = 1 \\ \infty & \text{for } \rho = -1. \end{cases} \quad (28)$$

Here, for $\rho = -1$, the MI $= \infty$ does not mean that one gets the infinite amount of information. Instead, it means that the true/ overall target information has been received. It is true that for $\rho = -1$ case, the noise components $w_1(t)$ and $w_2(t)$ cancel out each other. At the receiver, one has only the true information of the target.

2) MI IN MIXED-USE BAND

MI in a mixed-use band with multipath holds a similar procedure of MI in a clean environment. The only difference is, instead of using MI of the radar-only band in a clean environment, here, MI of the radar-only band with multipath defined in (27) is used here. The resulting MI similar to (16) is given by

$$I_{B_{mix}}^{max}(z_r(t); g(t) \mid x(t)) = \begin{cases} \bar{\epsilon}_1 & \left(TB_{mix} \ln D - T\int_{B_{mix}} \ln\left[r(f)\left(\frac{1+\rho}{2}\right)\right]df\right) \\ & \text{without SIC scheme} \\ \bar{\epsilon}_2 & \left(TB_{mix} \ln D - T\int_{B_{mix}} \ln\left[r(f)\left(\frac{1+\rho}{2}\right)\right]df\right) \\ & \text{with SIC scheme} \end{cases} \quad (29)$$

Finally, the MI of the SSR with multipath effect is given by

$$I_{B_{SSR}}^{max}(z_r(t); g(t) \mid x(t)) = I_{B_r}^{max}(z_r(t); g(t) \mid x(t)) + I_{B_{mix}}^{max}(z_r(t); g(t) \mid x(t)). \quad (30)$$

Here $I_{B_r}^{max}$ and $I_{B_{mix}}^{max}$ are defined in (27) and (29) respectively.

Similar to (18), the MI of the traditional radar with multipath is given by

$$I_{B_T}^{max}(z_r(t); g(t) \mid x(t)) = TB_T \ln D - T\int_{B_T} \ln\left[r(f)\left(\frac{1+\rho}{2}\right)\right]df \text{ (nats)}, \quad (31)$$

where D, $r(f)$ is defined in (38) and (6) respectively.

B. SE IN A MULTIPATH ENVIRONMENT

The SE of the SSR and traditional radar with multipath is same as (19) and (20), respectively. The main difference is that $I_{B_{SSR}}^{\max}$, $I_{B_T}^{\max}$ defined in (30), (31) is used here, instead of (17), (18). i.e.,

$$\text{SE}_{SSR} = \frac{I_{B_{SSR}}^{\max}}{B_{SSR}} \quad \text{and} \quad \text{SE}_T = \frac{I_{B_T}^{\max}}{B_T + B_{mix}}, \quad (32)$$

where $I_{B_{SSR}}^{\max}$, $I_{B_T}^{\max}$ are defined in (30), (31).

C. CAPACITY (C) IN A MULTIPATH ENVIRONMENT

In this subsection, the channel capacity of SSR in mixed-use band is calculated by considering the multipath effect between the in-band communication transmitter to SSR receiver. The bandlimited Gaussian channel capacity with a BW B_{mix}, effected with $w_1(t)$, $w_2(t)$ jointly Gaussian noise components with zero mean and covariance $K_w = \begin{bmatrix} \sigma_w^2 & \rho\sigma_w^2 \\ \rho\sigma_w^2 & \sigma_w^2 \end{bmatrix}$, $\sigma_w^2 = \frac{P_{ww}}{2}$, correlation coefficient ρ, and power P_c watts is given as [45]

$$C = B_{mix} \ln\left(1 + \frac{2P_c}{P_{ww}B_{mix}(1+\rho)}\right). \quad (33)$$

Using (33), similar to (22), the capacity of SSR in multipath environment is given by

$$C_{B_{mix}} = \begin{cases} \bar{\epsilon}_1 & B_{mix} \ln\left(1 + \frac{2P_c}{P_{ww}B_{mix}(1+\rho)}\right) \\ & \text{without SIC scheme} \\ \bar{\epsilon}_2 & B_{mix} \ln\left(1 + \frac{P_c}{P_{ww}B_{mix}(1+\rho)}\right) \\ & \text{with SIC scheme.} \end{cases} \quad (34)$$

V. RESULTS AND DISCUSSION

In this section, the numerical results are presented based on the analysis presented in Sections III and IV. In this framework, it is assumed that the SSR is operating at 3000 MHz with BW of 10 MHz. Also, it has the effective antenna area A_e of 2 m^2, and line of sight towards the target at 10 km range. The radar transmitter power varies from 50 W to 1000 W, and pulse duration varies from 0.1 ms to 100 ms. Here, the target scattering impulse response $g(t)$ has a Gaussian characteristics with spectral variance of

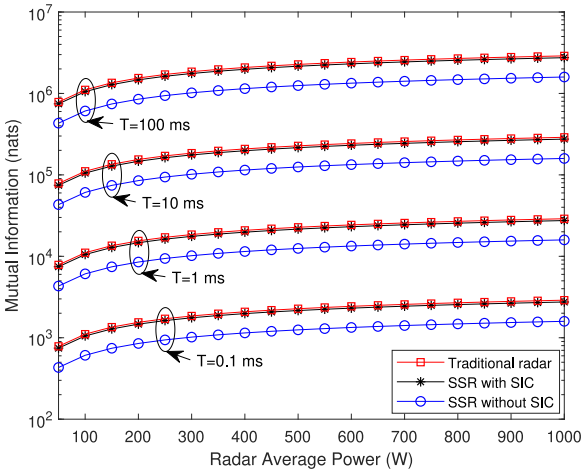

FIGURE 4. MI of SSR as a function of radar power and pulse duration assuming $B_{mix} = 50\%$ of B_{SSR}.

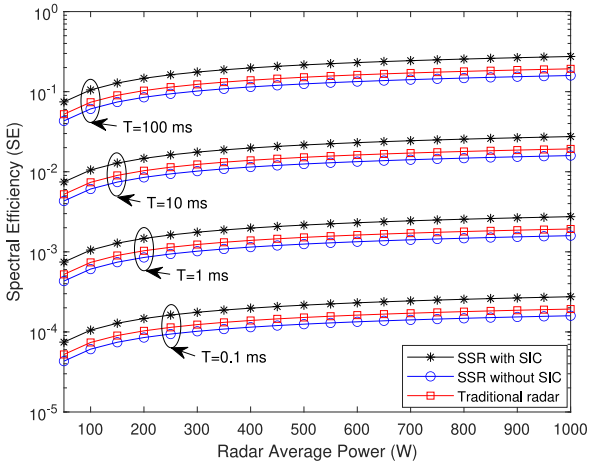

FIGURE 5. SE of SSR as a function of radar power and pulse duration assuming $B_{mix} = 50\%$ of B_{SSR}.

$\sigma_G^2(f) = B\exp\{-\delta f^2\}$. Here, B and δ are constant, characterize the magnitude and the rate of decrease of $\sigma_G^2(f)$ [41]. The SSR uses 50% of available BW for radar only operation and the rest for mixed-use purpose, until and unless specified. The additive noise $w(t)$ is white Gaussian having one-sided power spectral density $P_{ww}(f) = N_0 = kT_s$, with Boltzmann constant $k = 1.381 \times 10^{-23}$ J/K and system noise temperature $T_s = 300$ K. The communication system power varies from 5 W to 1000 W. From (14), (15), and (23), followed by the analysis there deduces the values of $\bar{\epsilon}_1$, $\bar{\epsilon}_2$ information reduction factors without using the SIC scheme and with using the SIC scheme [37], respectively in mixed-use band. Further, it is apparent that the $\bar{\epsilon}_1 \approx 0$ and $\bar{\epsilon}_2 \approx 1$. The same can also be verified for the values considered herein for the noise power, communication power and radar power. For the sake of analysis, $\bar{\epsilon}_1$ and $\bar{\epsilon}_2$ are considered as 0.1 and 0.9 respectively.

A. CLEAN ENVIRONMENT—USING EQUAL BW SHARING

The MI of the traditional radar and SSR are plotted in Figure 4, as a function of radar average power and pulse duration using (17) and (18). The power is varied from 50–1000 W with a step size of 100 W. Similarly, the pulse duration is varied from 0.1 ms to 100 ms with a step size of tenfold. In this analysis, 50% of total BW is allocated for the radar-only band and the rest for the mixed-use band. The MI is observed to increase with the increase in radar transmitted power and radar pulse duration. For a pulse duration of 100 ms, we observed that it outperforms the other smaller pulse duration values. Similarly, we observed that, for a given pulse duration, as the average power increase, the MI increases. This is because the higher the power impinges on the target, the more the information received. Further, it is evident from the results that MI of the traditional radar is always higher than the SSR due to the flexibility of using total available BW for radar-only purpose. Further, in SSR, the influence of using the SIC scheme in the mixed-use band is also depicted in the same Figure 4. We can see that the MI of SSR with the SIC is almost equal to that of the traditional radar because the SIC scheme in the mixed-use band cancels the in-band interference and ensures the maximum information retrieval in that band. Whereas in the absence of the SIC scheme, the target information retrieval becomes less and results in degraded MI of SSR as shown in the Figure 4. This is because we are losing the target information from the mixed-use band for an SSR radar when the SIC scheme is not adopted.

Figure 5 shows the SE of the traditional radar and SSR as a function of radar average power and pulse duration with $B_{mix} = 50\%$ of B_{SSR}. The analysis is based on (19) and (20). It can be observed from Figure 5, the SE is proportional to the radar transmitted power and radar pulse duration for a given BW. Even though the traditional radar MI is higher than the SSR (refer to Figure 4), whereas in the case of SE, the SSR with SIC stands higher than that of traditional radar. This is because the traditional radar accounts for additional BW of B_{mix} than the SSR for the same amount of information that needs to be obtained. Further, it is observed that the SE of the SSR without SIC is less compared to other schemes, owing to its poor information retrieval in mixed-use band.

Figures 6 and 7 show the MI and SE as a function of pulse duration and for a fixed radar power and equal BW sharing. The pulse duration is varied from 0.1 ms to 100 ms and a fixed radar power of 1000 W is considered. These plots are based on (17), (18), (19), and (20). It is observed that, as the pulse duration increases, both MI and SE values proportionately increases for the fixed radar power. It is because of the fact that, increase in pulse duration enhances energy per pulse and improves the target detection capability within the specified range. Therefore, the information retrieval will be higher, which in turn improves the SE.

B. CLEAN ENVIRONMENT—USING UNEQUAL BW SHARING

Figure 8 shows the MI of the traditional radar (always the BW is 100%) and SSR with unequal allocated BW (ex. radar

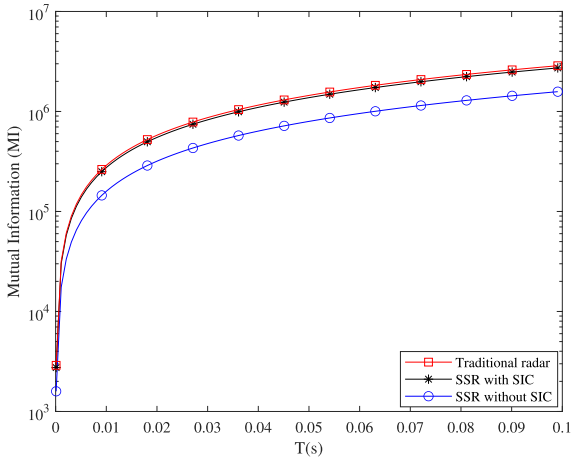

FIGURE 6. MI of SSR as a function of pulse duration.

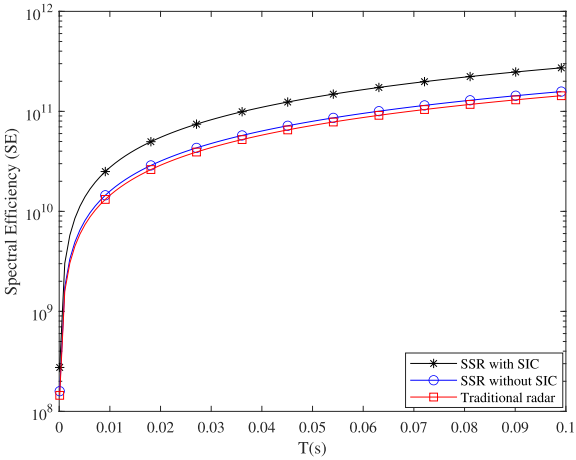

FIGURE 7. SE of SSR as a function of pulse duration.

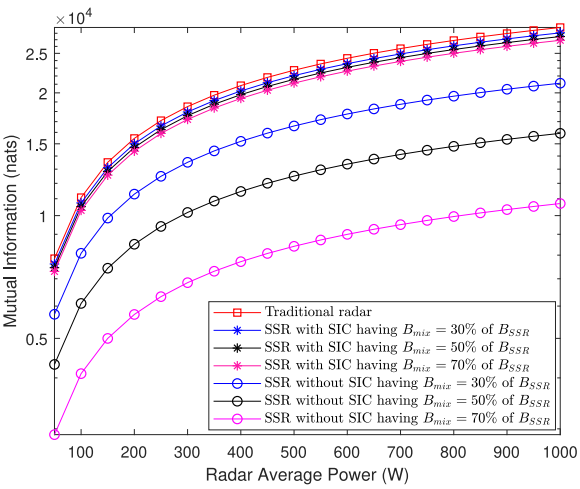

FIGURE 8. MI of SSR as a function of radar power and B_{mix} with a fixed pulse duration of 1ms.

band 30% and mixed band 70%). In this analysis, rather than varying the pulse duration, it is fixed to 1 ms, and the figures are plotted using (17) and (18). Three different

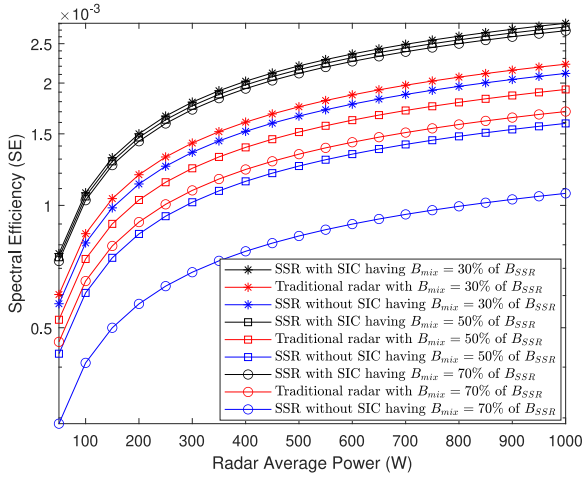

FIGURE 9. SE of SSR as a function of radar power and B_{mix} with fixed pulse duration of 1ms.

BW allocations are considered namely low mixed band BW (radar band 70% and mixed band 30%), equal BW (radar band 50% and mixed band 50%), and high mixed band BW (radar band 30% and mixed band 70%). From Figure 8, we can observe that MI of traditional radar is outperforming compared to other cases due to the availability of full BW, and there is no in-band interference. Whereas, MI of SSR with the SIC scheme is higher than the MI of SSR without SIC scheme in all the unequal BW sharing cases since the use of SIC scheme in mixed band retrieves more information. As the B_{mix} increases, the MI decreases and vice-versa. In support of this statement, it is clearly observed from the Figure 8, that the SSR with/without SIC having B_{mix} of 70% attains lesser MI compared to other cases. It is also worth noting that SSR with SIC also varies dominantly by changing the B_{mix}. But, this is not properly being visualized in the figures due to the $log - y$ scale. The rate of decrease of MI of SSR with respect to B_{mix} is less comparable in the case of SSR with the SIC scheme. At the same time, one can find a comparable decrease in the case of SSR without the SIC scheme. It is a fact that using larger B_{mix} and not using the SIC scheme in the mixed-use band leads to more information loss.

Similar to MI of Figure 8, the SE analysis is also carried out for traditional radar and SSR, as a function of average radar power, and B_{mix}, with a fixed pulse duration of 1 ms. Figure 9 shows the SE with unequal BW allocation, and is obtained based on (19) and (20). For the $B_{mix} = 30\%,\ 50\%,\ 70\%$ of B_{SSR}, the denominator of (20) becomes $1.3B_T$, $1.5B_T$, and $1.7B_T$ respectively. It is observed that the SE of SSR with the SIC scheme is higher than the traditional radar case, and SSR without the SIC case. In all the three proportions of mixed-use BW allocation (for $B_{mix} = 30\%,\ 50\%,\ 70\%$ of B_{SSR}), the order of the SE follows SE with SIC $>$ SE of traditional radar $>$ SE without SIC. The SE without SIC scheme falls below the other two cases (SE with SIC and traditional radar) in

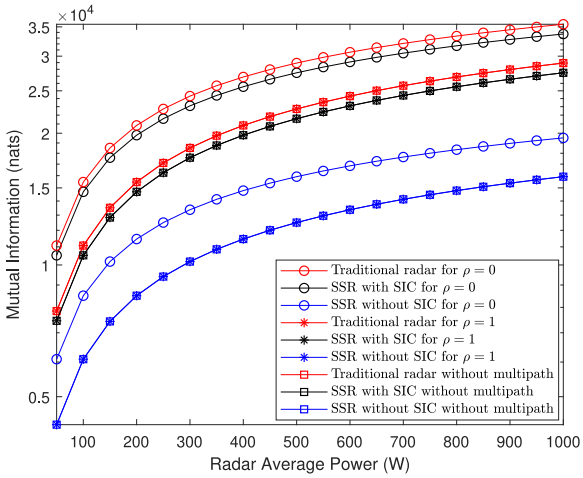

FIGURE 10. Comparison of MI of SSR for clean and multipath environment (B_{mix} = 50% of B_{SSR} and T = 1ms).

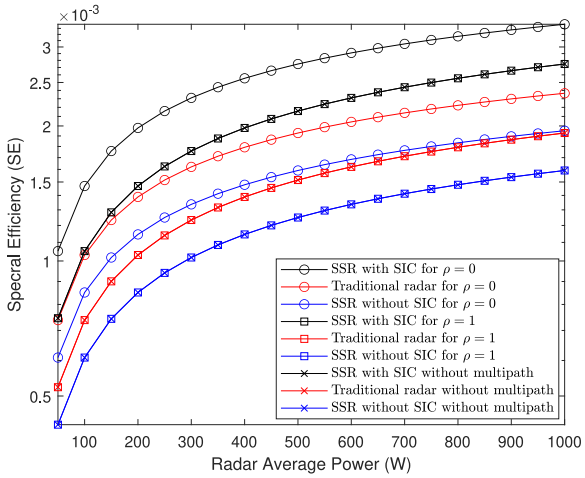

FIGURE 11. Comparison of SE of SSR for clean and multipath environment (B_{mix} = 50% of B_{SSR} and T = 1ms).

their corresponding proportion of allocated mixed-use BW. Further, it is noted that, the allocation of more amount of BW ($B_{mix} = 70\%$ of B_{SSR}) to the mixed-use band leads to the less SE of SSR without SIC case. Because the allocation of a high portion of total available BW for the mixed-use band and not being able to use the SIC scheme will result in considerable information loss, which inturn reflects on SE.

C. IMPACT OF MULTIPATH IN SSR

In the above Sections V-A and V-B, we considered the case of a clean environment and given detailed discussions on the impact of radar power, pulse duration, and allocation of unequal BW in SSR. The results obtained (Figures 4–9) in those sections hold true for multipath case. Hence, we avoid the Figures and summarize the results about multipath cases. In summary, the MI and SE increase with average radar power and pulse duration in multipath cases. Similarly, MI of traditional radar is higher than the SSR configuration, and SE of SSR is higher than the traditional radar. These results are not plotted again for the multipath case to eliminate the redundancy. Instead, the comparison results of clean environment and multipath environment are provided.

Figure 10 depicts the comparison of MI in a clean and multipath environment for both traditional and SSR. Here, we considered $B_{mix} = 50\%$ of B_{SSR}, and a fixed pulse duration of 1ms, based on (17), (18), (30), and (31). The impact of the correlation coefficient ρ is analyzed. It is observed that the MI of traditional radar and SSR with $\rho = 0$ is dominating compared to $\rho = 1$. This domination of SSR is theoretically true. Because, for $\rho = 0$, the jointly Gaussian noise components $w_1(t)$, $w_2(t)$ of two paths act as independent paths. Hence, the multipath target-to-receiver channel act like two looks Gaussian channel [45]. Therefore, the receiver has additional target information from multiple paths. Next, the MI of traditional and SSR in a multipath environment for $\rho = 1$ is equal to that of a clean environment. For $\rho = 1$, the multipath target-to-receiver channel acts like a single look Gaussian channel, same as the clean environment target-to-receiver channel model.

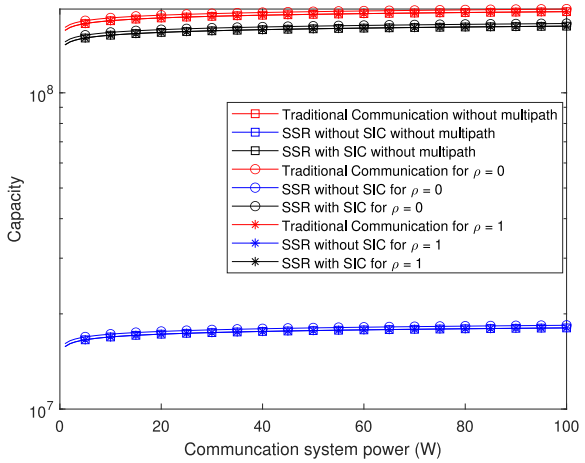

FIGURE 12. Comparison of capacity of SSR for clean and multipath environment (B_{mix} = 50% of B_{SSR}).

Figure 11 shows the comparison of SE of SSR and traditional radar in both clean and multipath environment having $B_{mix} = 50\%$ of B_{SSR} and a fixed pulse duration of 1ms. The results are obtained using (19), (20), (32). Similar to Figure 10, here it is observed that SE of traditional and SSR for $\rho = 0$ is higher compared to $\rho = 1$. Similarly, the SE for $\rho = 1$ case is equal to the SE of clean environment. Since the SE is directly proportional to MI, the change in MI directly reflects in SE.

Figure 12 shows the performance analysis of SSR from communication point of view by considering the capacity as a metric for performance evaluation. It shows the comparison between the capacity of SSR and the capacity of traditional communication system in both clean and multipath environment having $B_{mix} = 50\%$ of B_{SSR}. The results are obtained using (22) and (34). Similar to Figure 10, 11, it is observed that the capacity of traditional communication system and

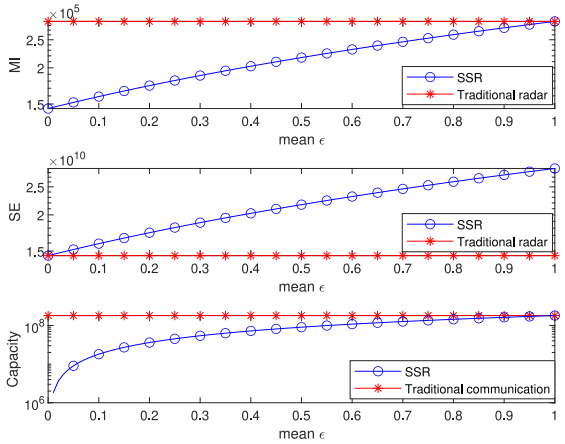

FIGURE 13. Comparison of MI, SE, and capacity (C) of SSR with varying mean ϵ.

SSR mode of operation for $\rho = 0$ is higher compared to $\rho = 1$. Because, for $\rho = 0$, both the paths become independent and contribute to the capacity constructively. Similarly, the capacity for $\rho = 1$ case is equal to the capacity of clean environment. Unlike MI and SE, the capacity of SSR with SIC and without SIC are considerably separated due to suppression of the interference by the SIC scheme. It is because the communication system capacity is only available in the mixed-use band. However, for the MI and SE metrics, both radar only band and mixed-use band contribute the target information.

Figure 13 shows the comparison of MI, SE, and capacity (C) of SSR with traditional systems by varying the mean ϵ. This figure also shows the impact of residual and direct interference components on the performance metrics MI, C, and SE. The Figure 13 is based on the generalized MI of SSR represented in (10) and its similar forms for SE and C. Let mean $\epsilon \approx 0$ is the SSR without SIC region or $\bar{\epsilon}_1$ region or direct interference region. Let mean $\epsilon \approx 1$ is the SSR with SIC region or $\bar{\epsilon}_2$ region or residual interference region. The region between these two direct and residual interference regions can be interpreted as a transition region. From (14), (15), and (23), the $\bar{\epsilon}_1$, $\bar{\epsilon}_2$ are related to direct and residual interference components, varying these quantities or observing the performance of SSR in the corresponding regions automatically quantifies the effect of direct and residual interference. It is observed that, the performance of the SSR without SIC region falls short when compared to traditional systems. However, it align with the traditional system with SIC region for MI and C metrics. It is because, the SSR without SIC region is the region where the direct interference will be present (referencing to (14) and (23)), which in turn deteriorates the information retrieval. Whereas in $\bar{\epsilon}_2$ region, the SSR uses the SIC scheme, results into the residual interference (referencing to (15) and (23)), which allows the better information reception. Further, the SSR provides improved performance for SE metric. The SE of SSR in without SIC region is similar to the SE of traditional system and SE of SSR with SIC scheme is superior compared with traditional systems.

VI. CONCLUSION

Spectrum sharing radar (SSR) has been considered in this paper, assuming that a portion of the bandwidth is allocated for radar-only purposes and the remainder for radar and communication purposes. The performance of the SSR has been analyzed in terms of mutual information (MI), spectral efficiency (SE), and capacity (C) metrics. These metrics are derived mathematically in a clean environment (no multipath) by considering SSR in the mixed-use band with and without a successive interference cancellation (SIC) scheme. Allocating a higher BW to the mixed-use band and employing the SIC scheme result in MI comparable to traditional radar. Similarly, for higher BW allocation to mixed-band, the SE of SSR outperforms conventional radar. The capacity of SSR in mixed-used and using SIC scheme reflects in comparable performance of traditional communication system. Later, the multipath environment is considered between the target and receiver channels and mathematically modified the MI, SE, and C metrics to account for it. The influence of the correlation coefficient ρ has also been investigated. The numerical results of the SSR in a clean and multipath environment are plotted in terms of MI, SE, and C and compared with the traditional radar and communication system. Results reveal that the MI and C of the SSR using the SIC scheme in the mixed-use band is comparable to that of traditional radar and communication system, respectively. However, the SE of the SSR with the SIC scheme is improved. Further, results reveal that the performance metrics of SSR with correlation factor zero dominates the unity correlation factor in multipath environment. Furthermore, the results show that not using the SIC scheme in a mixed-use band degrades SSR performance compared to traditional systems. These findings and analyses serve as a guideline for SSR designers. This work could be expanded to include the joint optimization of all performance metrics. Further, one can work on multiple SSR target scenarios with different target waveform response characteristics, introducing electronic countermeasures. Furthermore, this work can be extended to analyse the performance of SSR by introducing the multiple antennas at the receiver and considering N number of multi-paths into account. In addition, the future research work can also be carried out by evaluating the additional performance metrics such as detection probability etc for performance analysis.

APPENDIX

To maximize the $I_{B_r}(z_r(t); g(t) \mid x(t))$ with respect to transmit waveform energy constraint $\int_{B_r} |X(f)|^2 df = E_x$, form an objective function using the Lagrange multiplier theorem [48] as

$$\Psi\left(|X(f)|^2\right) = T \int_{B_r} \ln\left[1 + \frac{4|X(f)|^2 \sigma_G^2(f)}{P_{ww}(f) T(1+\rho)}\right] df - \lambda\left(\int_{B_r} |X(f)|^2 df - E_x\right) \tag{35}$$

The equivalent/ reduced objective function which needs to be maximized with respect to $|X(f)|^2$ is

$$\psi\left(|X(f)|^2\right) = T\ln\left[1+\frac{4|X(f)|^2\sigma_G^2(f)}{P_{ww}(f)T(1+\rho)}\right]-\lambda|X(f)|^2 \tag{36}$$

For maximization, take the partial differentiation of (36) with respect to $|X(f)|^2$ and equate it to zero. It is seen that,

$$|X(f)|^2 = D-\left(\frac{P_{ww}(f)T}{2\sigma_G^2(f)}\right)\left(\frac{1+\rho}{2}\right), \tag{37}$$

where $D=\frac{T}{\lambda}$ is some constant.

Using the energy constraint of $|X(f)|^2$ and (37), the value of D is given by

$$D=\frac{1}{B_r}\left[E_x+\int_{B_r}\left(\frac{P_{ww}(f)T}{2\sigma_G^2(f)}\right)\left(\frac{1+\rho}{2}\right)\right] \tag{38}$$

Using (6), (37), the maximum of $I_{B_r}(z_r(t);g(t)\mid x(t))$ is

$$\begin{aligned}
I_{B_r}^{max}(z_r(t);g(t)\mid x(t)) &= T\int_{B_r}\ln\left[1+\frac{4|X(f)|^2\sigma_G^2(f)}{P_{ww}(f)T(1+\rho)}\right]df\\
&= T\int_{B_r}\ln\left[1+\frac{D-\left[r(f)\left(\frac{1+\rho}{2}\right)\right]}{r(f)\left(\frac{1+\rho}{2}\right)}\right]df\\
&= T\int_{B_r}\ln D-\ln\left[r(f)\left(\frac{1+\rho}{2}\right)\right]df\\
&= TB_r\ln D-T\int_{B_r}\ln\left[r(f)\left(\frac{1+\rho}{2}\right)\right]df\ \text{(nats)},
\end{aligned} \tag{39}$$

where D is defined in (38).

REFERENCES

[1] G. Forecast et al., "Cisco visual networking index: Global mobile data traffic forecast update, 2017–2022," Cisco, San Jose, CA, USA, White Paper, 2019.

[2] B. Paul, A. R. Chiriyath, and D. W. Bliss, "Survey of RF communications and sensing convergence research," *IEEE Access*, vol. 5, pp. 252–270, 2017.

[3] M. L. Rahman et al., "Enabling joint communication and radar sensing in mobile networks—A survey," 2020, *arXiv:2006.07559*.

[4] M. Alaee-Kerahroodi, E. Raei, S. Kumar, and B. S. M. R. R, "Cognitive radar waveform design and prototype for coexistence with communications," *IEEE Sensors J.*, vol. 22, no. 10, pp. 9787–9802, May 2022.

[5] S. D. Blunt and E. S. Perrins, Eds., *Radar and Communication Spectrum Sharing*. London, U.K.: Inst. Eng. Technol., 2018.

[6] M. Labib, V. Marojevic, A. F. Martone, J. H. Reed, and A. I. Zaghloui, "Coexistence between communications and radar systems: A survey," *URSI Radio Sci. Bull.*, vol. 2017, no. 362, pp. 74–82, Sep. 2017.

[7] D. P. Zilz and M. R. Bell, "Statistical modeling of wireless communications interference and its effects on adaptive-threshold radar detection," *IEEE Trans. Aerosp. Electron. Syst.*, vol. 54, no. 2, pp. 890–911, Apr. 2018.

[8] N. Nartasilpa et al., "Let's share CommRad: Co-existing communications and radar systems," in *Proc. IEEE Radar Conf.*, Apr. 2018, pp. 1278–1283.

[9] J. A. Zhang et al., "An overview of signal processing techniques for joint communication and radar sensing," 2021, *arXiv:2102.12780*.

[10] Y. Gu, L. Zhang, Y. Zhou, and Q. Zhang, "Embedding communication symbols into radar waveform with orthogonal FM scheme," *IEEE Sensors J.*, vol. 18, no. 21, pp. 8709–8719, Nov. 2018.

[11] D. Gaglione et al., "Waveform design for communicating radar systems using fractional Fourier transform," *Digit. Signal Process.*, vol. 80, pp. 57–69, Sep. 2018.

[12] Y. Gu, L. Zhang, Y. Zhou, and Q. Zhang, "Waveform design for integrated radar and communication system with orthogonal frequency modulation," *Digit. Signal Process.*, vol. 83, pp. 129–138, Dec. 2018.

[13] R. Liu, M. Li, Q. Liu, and A. L. Swindlehurst, "Dual-functional radar-communication waveform design: A symbol-level precoding approach," *IEEE J. Sel. Topics Signal Process.*, vol. 15, no. 6, pp. 1316–1331, Nov. 2021.

[14] C. Xu, B. Clerckx, S. Chen, Y. Mao, and J. Zhang, "Rate-splitting multiple access for multi-antenna joint radar and communications," *IEEE J. Sel. Topics Signal Process.*, vol. 15, no. 6, pp. 1332–1347, Nov. 2021.

[15] D. P. Zilz and M. R. Bell, "Optimal linear detection of signals in cyclostationary, linearly modulated, digital communications interference," *IEEE Trans. Aerosp. Electron. Syst.*, vol. 55, no. 3, pp. 1123–1145, Jun. 2019.

[16] A. Khawar, A. Abdelhadi, and C. Clancy, "Target detection performance of spectrum sharing MIMO radars," *IEEE Sensors J.*, vol. 15, no. 9, pp. 4928–4940, Sep. 2015.

[17] J.-H. Lim, D.-W. Lim, B. L. Cheong, and M.-S. Song, "Spectrum sharing in weather radar networked system: Design and experimentation," *IEEE Sensors J.*, vol. 19, no. 5, pp. 1720–1729, Mar. 2019.

[18] Z. Wei, J. Zhu, Z. Guo, and F. Ning, "The performance analysis of spectrum sharing between UAV enabled wireless mesh networks and ground networks," *IEEE Sensors J.*, vol. 21, no. 5, pp. 7034–7045, Mar. 2021.

[19] P. Patel and J. Holtzman, "Analysis of a simple successive interference cancellation scheme in a DS/CDMA system," *IEEE J. Sel. Areas Commun.*, vol. 12, no. 5, pp. 796–807, Jun. 1994.

[20] K. Higuchi and A. Benjebbour, "Non-orthogonal multiple access (NOMA) with successive interference cancellation for future radio access," *IEICE Trans. Commun.*, vol. 98, no. 3, pp. 403–414, 2015.

[21] P. Setlur, N. Devroye, and M. Rangaswamy, "Radar waveform design with the two step mutual information," in *Proc. IEEE Radar Conf.*, 2014, pp. 1317–1322.

[22] G. Srinath, H. P. Kumar, P. Srihari, R. Tharmarasa, and T. Kirubarajan, "Coherent radar target detection with in-band cyclostationary wireless interference," *IEEE Access*, vol. 10, pp. 11173–11190, 2022.

[23] G. Srinath, B. Pardhasaradhi, P. K. H, and P. Srihari, "Tracking of radar targets with in-band wireless communication interference in RadComm spectrum sharing," *IEEE Access*, vol. 10, pp. 31955–31969, 2022.

[24] X. Yuan, Z. Feng, W. Ni, Z. Wei, and R. P. Liu, "Waveform optimization for MIMO joint communication and radio sensing systems with imperfect channel feedbacks," in *Proc. IEEE Int. Conf. Commun. Workshops (ICC Workshops)*, 2020, pp. 1–6.

[25] C. Aydogdu, M. F. Keskin, N. Garcia, H. Wymeersch, and D. W. Bliss, "RadChat: Spectrum sharing for automotive radar interference mitigation," *IEEE Trans. Intell. Transp. Syst.*, vol. 22, no. 1, pp. 416–429, Jan. 2021.

[26] W. Yuan, Z. Wei, S. Li, J. Yuan, and D. W. K. Ng, "Integrated sensing and communication-assisted orthogonal time frequency space transmission for vehicular networks," *IEEE J. Sel. Topics Signal Process.*, vol. 15, no. 6, pp. 1515–1528, Nov. 2021.

[27] A. Tang, S. Li, and X. Wang, "Self-interference-resistant IEEE 802.11ad-based joint communication and automotive radar design," *IEEE J. Sel. Topics Signal Process.*, vol. 15, no. 6, pp. 1484–1499, Nov. 2021.

[28] A. R. Chiriyath, S. Ragi, H. D. Mittelmann, and D. W. Bliss, "Novel radar waveform optimization for a cooperative radar-communications system," *IEEE Trans. Aerosp. Electron. Syst.*, vol. 55, no. 3, pp. 1160–1173, Jun. 2019.

[29] A. Hassanien, M. G. Amin, E. Aboutanios, and B. Himed, "Dual-function radar communication systems: A solution to the spectrum congestion problem," *IEEE Signal Process. Mag.*, vol. 36, no. 5, pp. 115–126, Sep. 2019.

[30] A. Ahmed, Y. D. Zhang, and Y. Gu, "Dual-function radar-communications using QAM-based sidelobe modulation," *Digit. Signal Process.*, vol. 82, pp. 166–174, Nov. 2018.

[31] C. G. Tsinos, A. Arora, S. Chatzinotas, and B. Ottersten, "Joint transmit waveform and receive filter design for dual-function radar-communication systems," *IEEE J. Sel. Topics Signal Process.*, vol. 15, no. 6, pp. 1378–1392, Nov. 2021.
[32] Q. Zhang, Y. Zhou, L. Zhang, Y. Gu, and J. Zhang, "Circulating code array for a dual-function radar-communications system," *IEEE Sensors J.*, vol. 20, no. 2, pp. 786–798, Jan. 2020.
[33] Z. Feng, Z. Fang, Z. Wei, X. Chen, Z. Quan, and D. Ji, "Joint radar and communication: A survey," *China Commun.*, vol. 17, no. 1, pp. 1–27, Jan. 2020.
[34] A. R. Chiriyath, B. Paul, G. M. Jacyna, and D. W. Bliss, "Inner bounds on performance of radar and communications co-existence," *IEEE Trans. Signal Process.*, vol. 64, no. 2, pp. 464–474, Jan. 2016.
[35] S. Gunnery, P. Bethi, P. H. Kumar, and S. Pathipati, "Target estimation performance improvement in cooperative radar and communication system spectrum sharing," in *Proc. 12th Int. Conf. Comput. Commun. Netw. Technol. (ICCCNT)*, 2021, pp. 1–6.
[36] T. Tian, T. Zhang, L. Kong, G. Cui, Q. Shi, and Y. Deng, "Performance of localization estimation rate for radar-communication system," in *Proc. IEEE Radar Conf.*, Apr. 2019, pp. 1–6.
[37] T. Tian, T. Zhang, L. Kong, G. Cui, and Y. Wang, "Mutual information based partial band coexistence for joint radar and communication system," in *Proc. IEEE Radar Conf.*, Apr. 2019, pp. 1–5.
[38] B. Wang and K. J. R. Liu, "Advances in cognitive radio networks: A survey," *IEEE J. Sel. Topics Signal Process.*, vol. 5, no. 1, pp. 5–23, Feb. 2011.
[39] T. Huang, N. Shlezinger, X. Xu, Y. Liu, and Y. C. Eldar, "MAJoRCom: A dual-function radar communication system using index modulation," *IEEE Trans. Signal Process.*, vol. 68, pp. 3423–3438, May 2020.
[40] K. Wu, J. A. Zhang, X. Huang, and Y. J. Guo, "Frequency-hopping MIMO radar-based communications: An overview," *IEEE Aerosp. Electron. Syst. Mag.*, vol. 37, no. 4, pp. 42–54, Apr. 2022.
[41] M. R. Bell, "Information theory and radar waveform design," *IEEE Trans. Inf. Theory*, vol. 39, no. 5, pp. 1578–1597, Sep. 1993.
[42] D. W. Bliss, "Cooperative radar and communications signaling: The estimation and information theory odd couple," in *Proc. IEEE Radar Conf.*, May 2014, pp. 50–55.
[43] Y. Rong, A. R. Chiriyath, and D. W. Bliss, "MIMO radar and communications spectrum sharing: A multiple-access perspective," in *Proc. IEEE 10th Sens. Array Multichannel Signal Process. Workshop (SAM)*, 2018, pp. 272–276.
[44] P. M. Woodward, *Probability and Information Theory, With Applications to Radar: International Series of Monographs on Electronics and Instrumentation*, vol. 3. Kent, U.K.: Elsevier, 2014.
[45] T. M. Cover and J. A. Thomas, *Elements of Information Theory*. Somerset, U.K.: Wiley, 2012.
[46] L. Deng, Y. Rui, P. Cheng, J. Zhang, Q. T. Zhang, and M. Li, "A unified energy efficiency and spectral efficiency tradeoff metric in wireless networks," *IEEE Commun. Lett.*, vol. 17, no. 1, pp. 55–58, Jan. 2013.
[47] A. R. Chiriyath, B. Paul, and D. W. Bliss, "Radar-communications convergence: Coexistence, cooperation, and co-design," *IEEE Trans. Cogn. Commun. Netw.*, vol. 3, no. 1, pp. 1–12, Mar. 2017.
[48] D. P. Bertsekas, *Constrained Optimization and Lagrange Multiplier Methods*. Cambridge, MA, USA: Academic, 2014.

GUNNERY SRINATH (Graduate Student Member, IEEE) received the B.Tech. degree in electronics and communication engineering from Jawaharlal Nehru Technological University, Anantapur, India, in 2013, the M.Tech. degree in digital communication from ABV-Indian Institute of Information Technology and Management at Gwalior, Gwalior, India, in 2016, and the Ph.D. degree in electronics and communication engineering from the National Institute of Technology Karnataka, Surathkal, Mangaluru, India, in 2023. From 2018 to 2019, he was a visiting Ph.D. student with the Estimation, Tracking and Fusion Research Laboratory, McMaster University, Hamilton, ON, Canada. He is currently working as a Technical Specialist with ADAS, Continental Autonomous Mobility India Pvt. Ltd., Bengaluru, India. His research interests include cognitive radio, radar signal processing, radar and communication system spectrum sharing, and target tracking.

BETHI PARDHASARADHI (Member, IEEE) received the B.Tech. degree in electronics and communication engineering from Jawaharlal Nehru Technological University Kakinada, Kakinada, India, in 2014, the M.Tech. degree in VLSI design from the ABV-Indian Institute of Information Technology and Management, Gwalior, India, in 2016, and the Ph.D. degree in electronics and communication engineering from the National Institute of Technology Karnataka, Mangaluru, India, in 2022. He was a Visiting Ph.D. Scholar for 16 months with Estimation Tracking and Fusion Laboratory, McMaster University, Hamilton, ON, Canada, under the supervision of Prof. T. Kirubarajan, from 2018 to 2019. He was a Visiting Researcher as part of Indo-Norwegian Collaboration to Autonomous and Cyber-Physical Systems Research Group, Department of Information and Communication Technology, University of Agder, Grimstad, Norway. He is currently working as a Technical Specialist with ADAS, Continental Autonomous Mobility India Pvt. Ltd., Bengaluru, India. His research interests include intentional interference to autonomous sensors, target tracking, and information fusion. He was a recipient of Sir C. V. Raman Award from the Institution of Engineering and Technology for Outstanding Academics and Research.

ASHOKA CHAKRAVARTHI MAHIPATHI (Graduate Student Member, IEEE) received the B.Tech. degree in electronics and communication engineering from Jawaharlal Nehru Technological University Kakinada, India, in 2009, and the M.Tech. degree in telecommunications from National Institute of Technology Durgapur, India, in 2012. He is currently pursuing the Ph.D. degree in electronics and communication engineering with the National Institute of Technology Karnataka, Surathkal, Mangalore, India. Later, he worked as an Assistant Professor with the Department of Electronics and Communication Engineering, K L University, Vijayawada, India, until June 2018. His research interests are in the area of cognitive radio, RF communications and sensing, optimum radar waveform design, and target tracking.

PRASHANTHA KUMAR H received the M.Tech. degree in digital electronics and communication from MIT Manipal, India, in 2001, and the Ph.D. degree in electronics and communication engineering from the National Institute of Technology Karnataka, Surathkal, India, in 2012. He was an Assistant Professor with the Department of Electronics and Communication Engineering, MIT Manipal for seven years. Since 2013, he has been with the National Institute of Technology Karnataka as an Assistant Professor. He is a Subject Expert in error control coding, wireless communication, signal processing for communication, and RF microelectronics. He is the author of MATLAB/Simulink for Digital Signal Processing (Seoul, South Korea, Hongrung Publishing Company) with Prof. W. Y. Yang.

PATHIPATI SRIHARI (Senior Member, IEEE) received the B.Tech. degree in electronics and communication engineering from Sri Venkateswara University, the master's degree in communications engineering and signal processing from the University of Plymouth, Plymouth, U.K., and the Ph.D. degree in radar signal processing from Andhra University in 2012. He worked as a Visiting Assistant Professor with McMaster University, Hamilton, ON, Canada, in 2014. He is currently working as an Assistant Professor with the National Institute of Technology Karnataka, Surathkal, India. His research interests include radar target tracking, radar waveform design, and efficient DSP algorithms for radar applications. He has received the 2010 IEEE Asia–Pacific Outstanding Branch Counselor Award and the Young Scientist Award from the Department of Science and Technology, New Delhi, for carrying out the sponsored research project entitled "Development of efficient target tracking algorithms in the presence of ECM." He is a Senior Member of ACM, a Fellow of IETE, and a member of IEICE, Japan.

LINGA REDDY CENKERAMADDI (Senior Member, IEEE) received the master's degree in electrical engineering from the Indian Institute of Technology Delhi, New Delhi, India, in 2004, and the Ph.D. degree in electrical engineering from the Norwegian University of Science and Technology (NTNU), Trondheim, Norway, in 2011.

He worked with Texas Instruments on mixed-signal circuit design before joining the Ph.D. Program with NTNU. After finishing the Ph.D. degree, he worked on radiation imaging for an atmosphere–space interaction monitor (ASIM mission to the International Space Station) with the University of Bergen, Bergen, Norway, from 2010 to 2012. He is currently the Leader of the Autonomous and Cyber-Physical Systems Research Group and a Professor with the University of Agder, Grimstad, Norway. He has coauthored over 120 research publications that have been published in prestigious international journals and standard conferences. His main scientific interests are in cyber–physical systems, autonomous systems, and wireless embedded systems.

Dr. Cenkeramaddi is also a member of the editorial boards of various international journals and the technical program committees of several IEEE conferences. He is the principal investigator and the co-principal investigator of many research grants from the Norwegian Research Council.